Antarctic Low-Tropospheric Humidity Inversions: 10-Yr Climatology

TIINA NYGÅRD AND TERESA VALKONEN

Finnish Meteorological Institute, and University of Helsinki, Helsinki, Finland

TIMO VIHMA

Finnish Meteorological Institute, Helsinki, Finland

(Manuscript received 15 July 2012, in final form 25 January 2013)

ABSTRACT

Humidity inversions are nearly permanently present in the coastal Antarctic atmosphere. This is shown based on an investigation of statistical characteristics of humidity inversions at 11 Antarctic coastal stations using radiosonde data from the Integrated Global Radiosonde Archive (IGRA) from 2000 to 2009. The humidity inversion occurrence was highest in winter and spring, and high atmospheric pressure and cloud-free conditions generally increased the occurrence. A typical humidity inversion was less than 200 m deep and 0.2 g kg^{-1} strong, and a typical humidity profile contained several separate inversion layers. The inversion base height had notable seasonal variations, but generally the humidity inversions were located at higher altitudes than temperature inversions. Roughly half of the humidity inversions were associated with temperature inversions, especially near the surface, and humidity and temperature inversion strengths as well as depths correlated at several stations. On the other hand, approximately 60% of the humidity inversions were accompanied by horizontal advection of water vapor increasing with height, which is also a probable factor supporting humidity inversions. The spatial variability of humidity inversions was linked to the topography and the water vapor content of the air. Compared to previous results for the Arctic, the most striking differences in humidity inversions in the Antarctic were a much higher frequency of occurrence in summer, at least under clear skies, and a reverse seasonal cycle of the inversion height. The results can be used as a baseline for validation of weather prediction and climate models and for studies addressing changes in atmospheric moisture budget in the Antarctic.

1. Introduction

Water vapor has an important role in the global climate system as it is the dominant greenhouse gas and notably affects the surface energy budget through cloud formation and radiative fluxes. The atmospheric water vapor content typically decreases toward higher latitudes and has its minimum in the polar areas. In the Antarctic, water vapor has traditionally been considered to have a rather passive role in the dynamics of the atmosphere, but it has received growing attention due to its importance to the mass balance of the continental ice sheets, associated with the concern of sea level rise (King and Turner 1997). Furthermore, it is recognized that possible changes in atmospheric water vapor and clouds, and their interactions with radiation, may play a key role in climate change in the Antarctic (Bromwich et al. 2012).

The atmospheric moisture budget over the Antarctic is largely governed by the horizontal water vapor transport (Tietäväinen and Vihma 2008). Several authors have provided estimates for the transport in the Antarctic based on radio soundings (Bromwich 1988; Connolley and King 1993), satellite data (Slonaker and Van Woert 1999), surface observations (Giovinetto et al. 1992, 1997), and reanalyses (Cullather et al. 1998; Tietäväinen and Vihma 2008; Cullather and Bosilovich 2011). Many of these studies have demonstrated that the transient eddies are the dominant contributors to the horizontal water vapor flux. It is also known that interannual and interdecadal variability of the water vapor transport in the Antarctic is noticeable and is associated with large-scale circulation patterns, such as the southern annular mode (SAM) and the zonal wave 3 (Tietäväinen and

Corresponding author address: Tiina Nygård, Finnish Meteorological Institute, P.O. Box 503, FI-00101 Helsinki, Finland.
E-mail: tiina.nygard@fmi.fi

DOI: 10.1175/JCLI-D-12-00446.1

Vihma 2008). In addition, spatial differences in the water vapor transport and the total column moisture are large; the most extreme conditions are found in the Antarctic Peninsula and the high plateau.

The saturation pressure of water vapor is strongly controlled by temperature and, therefore, humidity in the atmosphere typically decreases with height. Humidity inversions (i.e., layers where the specific humidity increases with height) are, however, common features in the lower troposphere in the polar areas (Curry et al. 1996; Devasthale et al. 2011; Vihma et al. 2011a). Factors that are known to contribute to humidity inversions can roughly be divided into two categories: 1) processes that are sources/sinks to the water vapor content of the atmospheric column and 2) processes that redistribute the water vapor content in the column. The temperature control of saturation pressure belongs to the first category, as it leads to condensation of excessive moisture to the surface or in the air. This can consequently create local minima in the vertical humidity profile depending on the shape of the temperature profile. Hence, the temperature control is also closely connected to temperature inversions. In earlier studies, temperature inversions have been found to be associated with humidity inversions in observations from the Arctic (Tjernström et al. 2004; Devasthale et al. 2011; Sedlar et al. 2012) and in model simulations from the Antarctic (Tastula et al. 2012). In addition to condensation, horizontal advection of water vapor, which may vary with altitude, can also cause direct changes in the water vapor content in the atmospheric column. On the other hand, turbulent mixing and large-scale vertical motions belong to the second category since they can redistribute the water vapor in the column but not directly reduce the water vapor content (Curry 1983).

Recent studies have demonstrated that humidity inversions have significant implications for cloud growth and persistence. Sedlar et al. (2012) and Solomon et al. (2011) concluded that a humidity inversion at a cloud top can be a moisture source to the cloud layer in the Arctic. This is made possible by turbulent motions or other dynamic instabilities near the cloud top, which can result in entrainment (Sedlar et al. 2012). Occasionally, when moisture from the surface layer is not efficiently transported into the mixed layer, humidity inversions can be the only source of moisture for the cloud system (Solomon et al. 2011). Hence, the humidity inversions can contribute to keep the lowest troposphere at a high relative humidity and cloud cover extensive (Devasthale et al. 2011). Further, Devasthale et al. (2011) discussed the influence of humidity inversions on the downwelling longwave radiation. Based on radio soundings from the Arctic, they found that when the atmospheric column was relatively dry, the humidity inversion contributed up to 50% of the total amount of condensed water vapor in a column, and when the atmospheric column was humid the contribution was often less than 15%. Since 70%–90% of the downwelling longwave radiation to the surface is emitted from the lowest 1000 m in the atmosphere (Ohmura 2001), Devasthale et al. (2011) concluded that humidity inversions have potentially significant impact on the radiative characteristics of the atmosphere.

Although humidity inversions potentially have an important influence on the climate, they have received little attention until now. Previous studies on humidity inversions have focused on the Arctic (Curry 1983; Sedlar and Tjernström 2009; Devasthale et al. 2011; Solomon et al. 2011; Vihma et al. 2011a; Kilpeläinen et al. 2012; Sedlar et al. 2012), and the Antarctic humidity inversions have remained largely neglected. In earlier decades, studies on water vapor were restricted by the low reliability of humidity sensors in a cold environment, but the quality of the measurements has improved significantly during the last decades (Miloshevich et al. 2006), allowing for climatological studies.

In this paper, we present climatology of humidity inversions over the Antarctic for the first time to our knowledge. The analysis is based on radiosonde data from an enhanced version of the Integrated Global Radiosonde Archive (IGRA) (Durre et al. 2006; Durre and Yin 2008) from 11 Antarctic coastal stations during the period 2000–09. We address the seasonal and spatial variability of humidity inversion occurrence, strength, depth, and base height, and compare our findings to previous results from the Arctic. We aim to answer the following questions: 1) How frequently do humidity inversions occur in the Antarctic? 2) How much do the occurrence and properties of humidity inversion vary temporally and spatially? 3) What are the roles of temperature inversions and moisture advection in supporting and shaping the humidity inversions? 4) Is the climatology of humidity inversions in the Antarctic different from the Arctic? We aim to provide results that can be used as a baseline for validation of weather prediction and climate models and for studies addressing changes in the atmospheric moisture budget in the Antarctic.

2. Data and analysis methods

a. Radio soundings

We utilized radiosonde data from the enhanced version of IGRA from circumpolar stations near the coast of Antarctica. IGRA is a comprehensive, freely available

global dataset of quality-assured radiosonde observations (Durre et al. 2006). In addition to the common radio sounding variables (pressure, temperature, dewpoint depression, wind speed, and wind direction), the enhanced version includes several derived variables such as geopotential height, potential temperature, water vapor pressure, and relative humidity (Durre and Yin 2008). The IGRA data are provided at the mandatory pressure levels specified by the World Meteorological Organization (WMO), including the surface level, and also at significant levels at which a sounding variable deviates from the linearity between two mandatory levels. Because the deviation points are included in IGRA, the actual shape of profiles is captured and no information of inversions is lost. The IGRA data, especially temperature profiles, have undergone rigorous quality assurance checks; a detailed description of these procedures is given in Durre et al. (2006). In this study, mainly the humidity profiles were analyzed. In addition, other sounding variables and synoptic cloud observations (fractions of low, middle, and high clouds, total cloud cover, and roughly estimated cloud base height) from the Reference Antarctic Data for Environmental Research (READER) at 3-h interval were used to interpret the humidity characteristics.

We selected the 10-yr period 2000–09 for the analyses. Traditionally, a 10-yr period is considered to be fairly short for climatological studies, but with this choice we could minimize the inhomogeneities resulting from changes in instrumentation or operation practices and the errors related to older humidity sensor types. During the study period, the SAM index was mostly positive and higher than during the previous decades. Tietäväinen and Vihma (2008) have shown that the total column water vapor and the zonal water vapor transport in the Antarctic correlate positively with the SAM index. Hence, our results on humidity characteristics represent relatively moist conditions during a positive SAM.

The study area was chosen to cover the circumpolar coast of the Antarctic where the water vapor transport is relatively large and errors in the humidity data are smaller than in the inland. The latter is due to very low inland temperatures that make humidity measurements more liable to errors. In IGRA, data from 11 Antarctic coastal stations were available for the whole study period, and these sites were selected for the analysis. The locations of the stations are shown in Fig. 1. The coverage of the stations was relatively good along the coast of East Antarctica, but only one station from the West Antarctica, Marambio, was included in the study. Marambio is located on an island at the tip of the Antarctic Peninsula and it represents a much milder and moister climate than the rest of the stations. In East Antarctica, Halley and

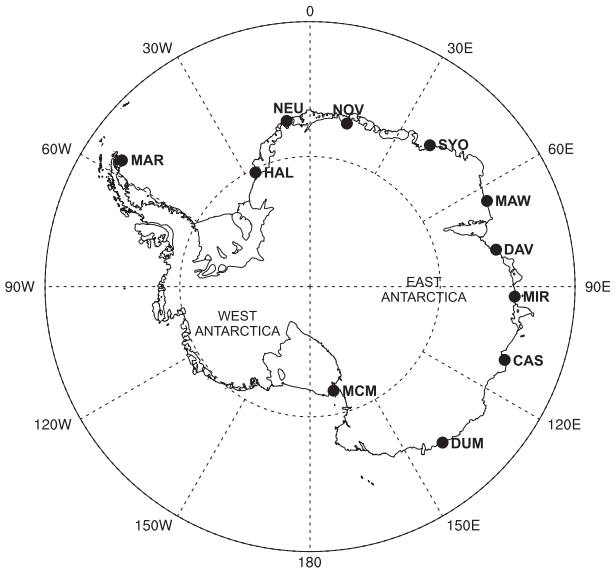

FIG. 1. Locations of the radio sounding stations. The full station names are listed in Table 1.

Neumayer are located on an ice shelf while the other stations are affected by a more complex topography. The heights of the stations and the radio sounding systems used are listed in Table 1. For further details of stations and their meteorological conditions, see Turner and Pendlebury (2004). Figure 2 illustrates how the data at each station were distributed in space and time. At all stations, the data were fairly evenly distributed between years and months, but the diurnal observation times were clustered around 0000 and 1200 UTC. Hence, the solar time of the observations varied largely between the stations as they are located at different longitudes (Fig. 2c), and therefore we did not analyze the diurnal cycle. The fraction of night/early morning soundings was large at Novolazarevskaya and Mirny in particular. In total, Marambio had notably fewer observations available than the other stations but it was included in the study as the temporal distribution of the data was similar to the other stations.

b. Reanalysis dataset

To get estimates for horizontal water vapor advection at the stations, the European Centre for Medium-Range Weather Forecasts (ECMWF) Interim Re-Analysis (ERA-Interim; Dee et al. 2011) was utilized. The reanalysis data were obtained at $0.72° \times 0.72°$ latitude–longitude resolution from 16 pressure levels between 1000 and 500 hPa and they covered the period 2000–09 at 6-h intervals. The ERA-Interim was chosen for this study as it has been found to provide the most realistic depiction of precipitation changes in the high southern latitudes

TABLE 1. Abbreviations of station names, station heights above sea level, coordinates, and radiosonde types used at the stations in 2000–09.

Station	Abbreviation	Height (m)	Coordinates	Radiosonde system
Marambio	MAR	198	64.2°S, 56.7°W	Vaisala R80
Halley	HAL	31	75.5°S, 26.6°W	Vaisala RS80–15G
Neumayer	NEU	50	70.7°S, 8.3°W	Vaisala R80
Novolazarevskaya	NOV	140	70.8°S, 11.8°E	Russia-USSR MRZ-3A
Syowa	SYO	15	69.0°S, 39.6°E	Japan Mensei RSII-80/RSII-91
Mawson	MAW	15	67.6°S, 62.8°E	Vaisala RS80–18G/RS80–15G/RS92-SGP
Davis	DAV	12	68.6°S, 78.0°E	Vaisala RS80–15G/RS92-SGP
Mirny	MIR	59	66.6°S, 93.0°E	Russia-USSR MARS-2–2/Russia-USSR MRZ-3A
Casey	CAS	41	66.3°S, 110.5°E	Vaisala RS80–18G/RS80–15G/RS92-SGP
Dumont d'Urville	DUM	43	66.7°S, 140.0°E	Vaisala R80
McMurdo	MCM	24	77.9°S, 166.7°E	Vaisala R92

(Bromwich et al. 2011). The radiosonde observations from the 11 coastal stations were assimilated into the model system through a four-dimensional variational data assimilation (4DVAR), which has significantly improved the analysis for those locations. Even though the reanalyses might generally be sensitive to changes in the observing system (Bengtsson et al. 2004), ERA-Interim does not reveal any artificial trends or spurious discontinuities in the high southern latitudes (Bromwich et al. 2011).

3. Methods

First, vertical profiles of specific humidity were calculated from the observed water vapor pressure and air pressure profiles from the surface to the 500-hPa level. Despite the rigorous quality checks made for the IGRA data (section 2a), the humidity data of IGRA may still suffer from errors, particularly in cold, dry conditions. Tomasi et al. (2006) presented error estimates for radiosonde humidity in the inland station Dome C in the Antarctic. They reported an average dry bias of 5%–10% in relative humidity for the Vaisala RS80-A and RS80-H Humicap sensors, and smaller percentages for the Vaisala RS90 and RS20 sensors. The errors (e.g., bias and time lag) thus vary with the sensor type. Because of different radiosonde types (Table 1) and operation practices used at different stations, we did not attempt any general humidity corrections for the data. However, to reduce the errors we excluded from the analysis the humidity profiles (from the surface to the 500-hPa level) in which the temperature was below −40°C and the relative humidity below 20% or in which the specific humidity was below 0.02 g kg^{-1}. Generally, the errors in this study are expected to be smaller than estimated by Tomasi et al. (2006) as our study was focused on the Antarctic coast.

Next, all the specific humidity inversion layers were identified and analyzed. The terminology used to define humidity inversions follows Vihma et al. (2011a). The humidity inversion depth is the difference between the base height, where specific humidity starts to increase with altitude, and the top height, where the specific humidity starts to decrease. The heights in this study were defined to be above the ground/snow level. The humidity inversion strength, in turn, is the difference in specific humidity between the inversion top and base. All the humidity inversions deeper than 10 m were selected for this study and no other limitations were set. Inversion layers separated by a layer of a negative lapse rate were considered to be separate inversion layers. Temperature inversions were identified using a definition and terminology analogous to humidity inversions. However, cases where the temperature change through the inversion was 0.3°C or less were ignored as in Kilpeläinen et al. (2012). Inversions were defined to be

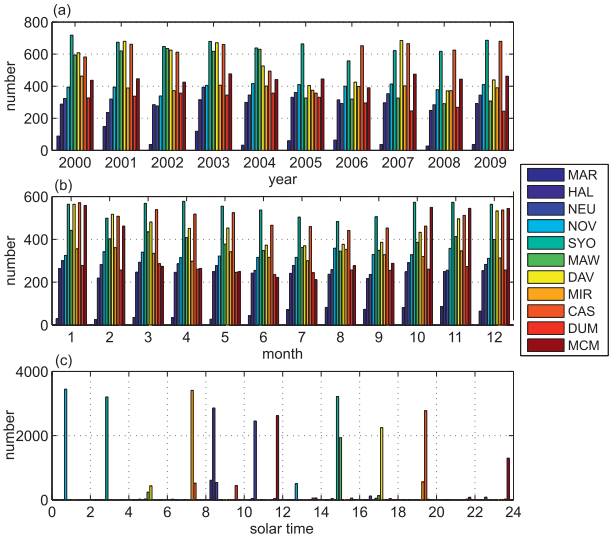

FIG. 2. Number of radiosonde observations per (a) year, (b) month, and (c) solar hour at the 11 Antarctic stations. The solar times in (c) are shown for bin intervals of 2 h.

surface based if the base was located below an altitude of 50 m.

Most previous studies on humidity and temperature inversions have been restricted to few fixed altitudes (Devasthale et al. 2011; Medeiros et al. 2011; Pavelsky et al. 2011) or clear-sky conditions (Devasthale et al. 2011) or have addressed only the strongest inversion in each profile (Devasthale et al. 2011). This study, however, was not limited to fixed levels, as the full vertical resolution of the radio sounding data was utilized. We present climatology for all humidity inversions, not only for the strongest one in a profile. Potentially, our approach of analyzing all individual humidity inversions separately could have concealed vertically deep inversions composed of several thin inversion layers. Zhang et al. (2011) reported that climatological temperature inversion statistics were not sensitive to threshold thickness of accepted embedded noninversion layers. To evaluate the sensitivity in case of humidity inversions, we did a test in which up to 200-m-deep layers with a negative lapse rate were allowed to be embedded within the inversion layer. The median number of humidity inversions in a profile decreased by 0.4 (16%) and the inversion depth increased by 24 m (9%), but the median inversion strength remained the same. It can thus be concluded that the climatological statistics presented in this study are not particularly sensitive to the inversion definition, and a large majority of humidity inversions were not part of any deeper inversion layer but were truly independent and vertically separate.

After inversions were identified, statistics of air humidity, and especially humidity inversions, were calculated. Since many of the humidity variables have positively skewed distributions, the arithmetic mean may notably be affected by a few individual data values. Therefore, we mostly paid attention to median values. To examine seasonality, the data were divided into four seasons. Transitional seasons (i.e., autumn and spring) are very short in the Antarctic, and the standard classification of 3-month seasons applied by climatologists is, therefore, not fully appropriate (King and Turner 1997). To better account for the nature of Antarctic climate, we adopted an objective definition of the seasons derived by Périard and Pettré (1993), which is based on a cluster analysis to temperature averages from Dumont d'Urville. Although this definition might not be perfect for the other Antarctic stations, it is certainly more realistic than the 3-month season classification. By the chosen definition, winter ranges from May to mid-October, spring from mid-October to mid-November, summer from mid-November to February, and autumn from March to April.

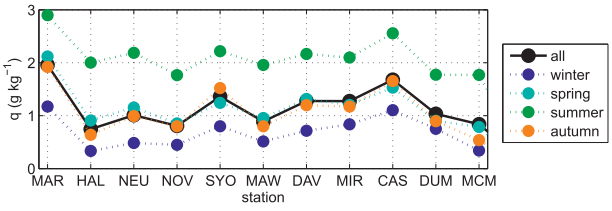

FIG. 3. Median of near-surface specific humidity for the whole 10-yr period and for each season separately.

Finally, relationships of temperature inversions and moisture transport to humidity inversions were investigated. This was motivated by previous studies (Curry 1983; Devasthale et al. 2011) that suggested that the temperature inversion and water vapor advection may be important contributors to humidity inversions in the Arctic. These relationships were investigated separately, however, keeping in mind that they are not always physically independent. Vertical profiles of horizontal water vapor advection were derived from the specific humidity and wind data of ERA-Interim for 11 station locations, and the difference in water vapor advection between the base and top height of radiosonde-based humidity inversions was calculated. Unfortunately, direct validation of ERA-Interim water vapor advection profiles was not possible given the sparse observation network in the Antarctic. Validation of specific humidity profiles, on the other hand, showed a root-mean-square error (RMSE) of approximately 0.3–0.4 g kg^{-1}, which was relatively constant with height and between the stations. The low variability of specific humidity RMSE hints that advection profiles derived from ERA-Interim are reasonable, and the reanalyses represent the best information on advection currently available.

4. Results

a. Statistical characteristics of humidity inversions

Although the atmosphere is relatively dry in the Antarctic, specific humidity had notable temporal and spatial variability. In Fig. 3, median surface (~2 m) specific humidity of the soundings is shown for all the stations. The decadal median varied between 0.8 and 2.0 g kg^{-1}, having a maximum at Marambio and minima at Halley and McMurdo. The difference between winter and summer median was on average 1.4 g kg^{-1}. Hence, the seasonal variability of the near-surface specific humidity was slightly larger than the spatial variability.

The vertical distribution of water vapor varied largely between the stations. Figure 4 illustrates the relative frequency distribution (RFD) of normalized specific

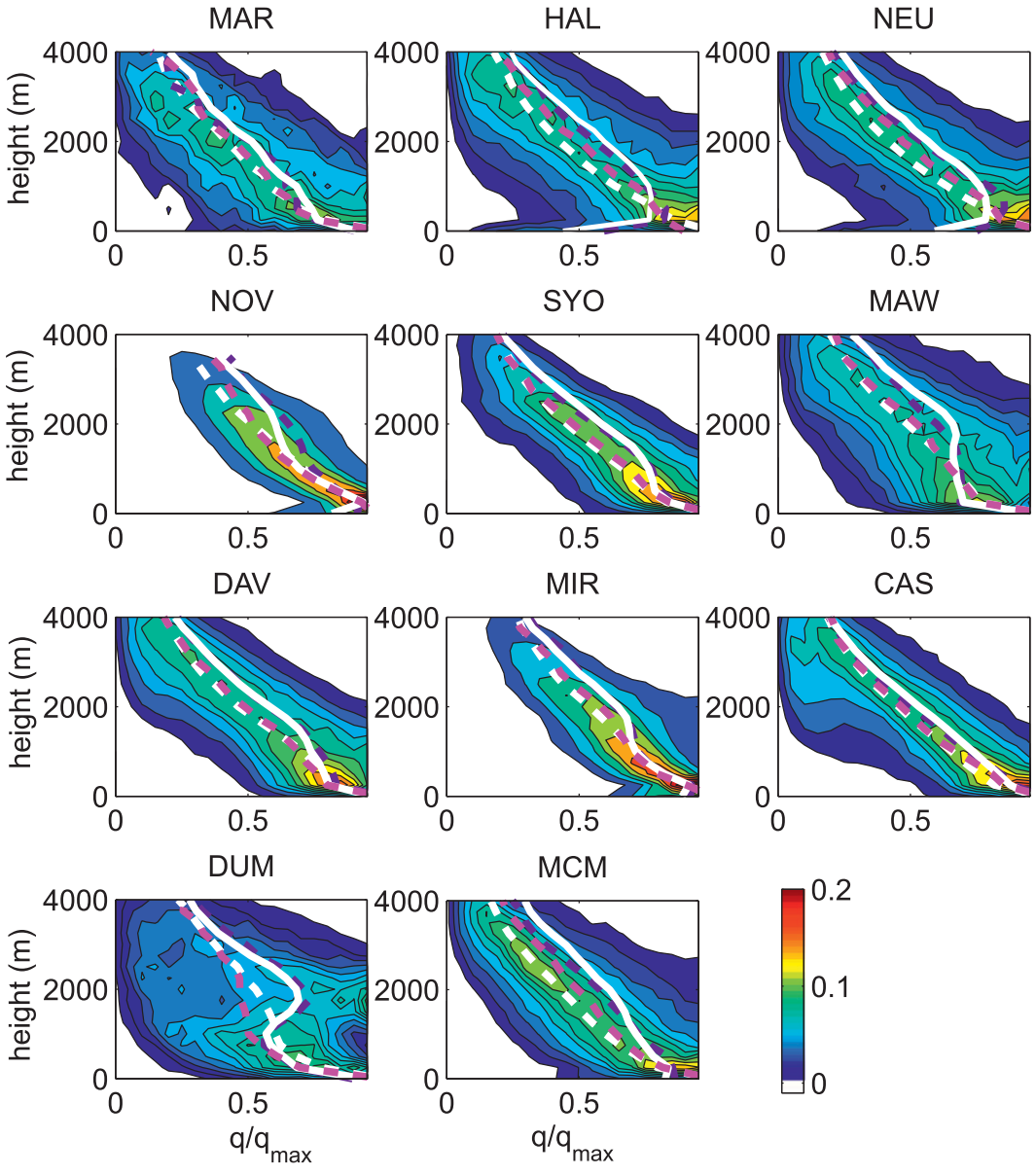

FIG. 4. Relative frequency distributions (RFDs; color scales, fraction) of normalized specific humidity (q/q_{max}) profiles. The lines denote season medians: winter (white solid line), spring (red dashed line), summer (white dashed line), and autumn (purple dashed line). The bin size is 0.05 and 250 m.

humidity profiles. The normalized specific humidity points out the altitude of the maximum specific humidity in a profile and shows the relative change of specific humidity with height. Especially at Dumont d'Urville, Mawson, and Halley, the profiles had a large scatter, whereas particularly at Novolazarevskaya and Mirny they had much narrower distribution. The latter may at least partly be due to the large fraction of nighttime soundings (Fig. 2). Dumont d'Urville and Mawson typically had a specific humidity maximum right at the surface (Fig. 4), and the relative humidity was also high near the surface. This can probably be explained by strong katabatic winds particularly experienced by these stations (Turner and Pendlebury 2004), which cause mixing of the air near the surface (Vihma et al. 2011b). Moreover, a consistent, elevated humidity inversion layer was seen in winter and autumn at Dumont d'Urville and Mirny at 1000–2000-m altitude and it is visible in Fig. 4. The altitude of these consistent elevated humidity inversions matched with the height of elevated temperature inversions at these stations.

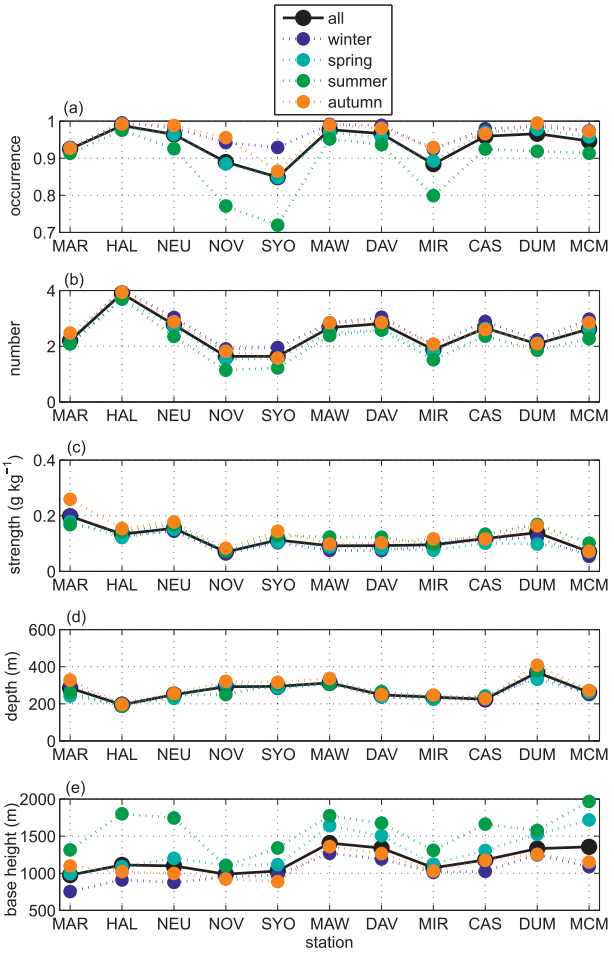

FIG. 5. (a) Occurrence of humidity inversions, (b) mean number of humidity inversions in a profile, and (c) median strength, (d) median depth, and (e) median base height of all humidity inversions.

Throughout the year, the occurrence of humidity inversions was very high (Fig. 5a); at most of the stations it was well above 0.9. Three of the stations (Novolazarevskaya, Syowa, and Mirny) showed marked seasonal variation of the inversion occurrence. Further, multiple inversion layers were very common at all the stations. Typically a profile from the surface to the 500-hPa altitude contained 2–4 humidity inversions (Fig. 5b). The number of inversions was typically smallest in summer and highest in winter; however, the seasonal variability was smaller than the spatial one. The inversion strength and depth (Figs. 5c,d) also showed surprisingly little seasonal variation, but varied more between the stations. In many respects, the spatial distribution of inversion strength followed the near-surface specific humidity shown in Fig. 3, indicating that where the humidity content of the air is high, humidity inversions can consequently be stronger. The median

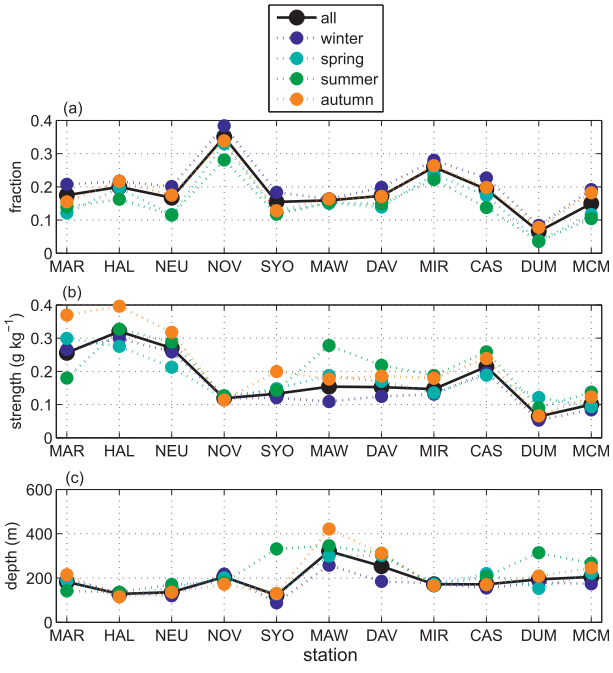

FIG. 6. (a) Fraction, (b) median strength, and (c) median depth of surface-based humidity inversions.

strength of the strongest inversion in a profile was twice as large as the median of all inversions. The median base height of all inversions was typically located at around 1000 m in winter and 1500 m in summer (Fig. 5e) while the base of the strongest inversion in each profile was typically located lower; at Halley the strongest humidity inversion of a profile was commonly found right at the surface, but elsewhere it was commonly elevated (not shown).

On average, 19% of all humidity inversions were classified as surface-based inversions (Fig. 6a), whereas the fraction of surface-based temperature inversions of all temperature inversions was 29%. This demonstrates that studies of Antarctic humidity inversions should not be limited to surface-based inversions only as the majority of humidity inversions are elevated. Seasonal variation of the fraction of surface-based humidity inversions was very small compared to the differences between the stations. The fraction was highest (35%) at Novolazarevskaya and smallest at Dumont d'Urville (7%). The strongest surface-based humidity inversions were found at Halley and Neumayer, which are both located on an ice shelf. All the other stations are, in turn, affected by a more complex topography. The surface-based inversions were generally stronger than the elevated inversions at all stations except for Dumont d'Urville (Figs. 5c and 6b). However, the depth of surface-based inversions was 80 m lower than the depth of elevated inversions (Figs. 5d and 6c).

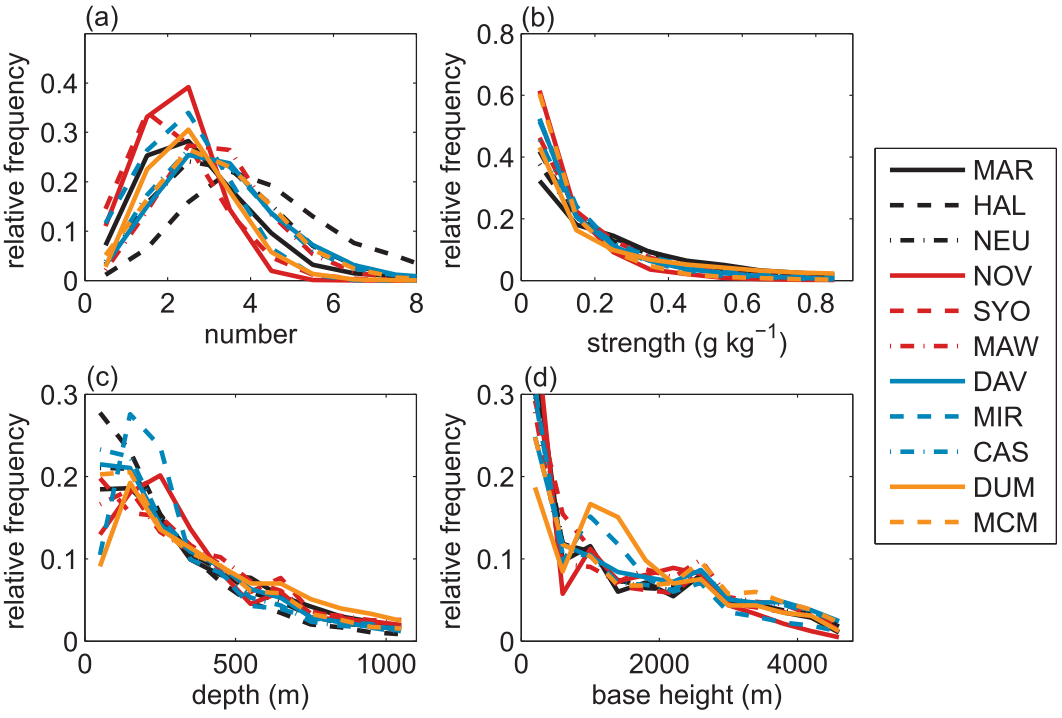

FIG. 7. RFDs of (a) number of humidity inversions in a profile, (b) inversion strength, (c) inversion depth, and (d) inversion base height. Bin sizes used in RFDs are 1 for the number, 0.1 g kg^{-1} for the strength, 100 m for the depth, and 200 m for the base height.

The range of temporal variability of humidity inversion properties was quite similar at all the stations, as illustrated in Fig. 7. RFDs of humidity inversion properties for the different seasons are not shown separately as seasonal variability in the RFDs was small. The number of humidity inversions in a profile had the largest spread at Halley, and the smallest at Novolazarevskaya and Syowa (Fig. 7). This can be connected to spatial differences in directional consistency of wind, defined as the ratio of the vector mean wind speed to the scalar mean. At Halley the directional constancy was 0.7 near the surface while at Novolazarevskaya and Syowa it reached 0.9. In other words, the origin of flow, and therefore also the origin of moisture, varied much more at the stations not experiencing strong katabatic flows. The strength distribution was nearly uniform at all stations, having almost an exponential shape, but the depth distribution had slightly more variation between the stations. The base height, in turn, had clear frequency peaks at several altitudes; the clearest of these were approximately at 1000 and 2500 m. Especially at Dumont d'Urville and Mirny these frequency peaks above 1000 m were notable.

Cloud cover had a relatively weak relationship with the humidity inversion as illustrated in Fig. 8, in which the statistics are shown for overcast (cloud fraction = 8/8) and clear-sky (cloud fraction $\leq$ 2/8) conditions. Nevertheless, the relationship with cloud cover was still statistically significant at many of the stations based on the Mann–Whitney U test (Fig. 8). The relationship between cloud cover and humidity inversion depth was not consistent and varied between the stations. On the other hand, the occurrence, number, and strength of inversions were consistently, although slightly, decreased in overcast conditions. At Mirny the humidity inversion occurrence frequency was nearly 0.2 lower in overcast conditions while other stations experienced a smaller influence of clouds. Dumont d'Urville, in turn, was the only station where the humidity inversion base was located at a lower level in overcast conditions. There, humidity inversion layers in overcast conditions were also deeper than in clear-sky conditions. When only surface-based humidity inversions were considered, the inversion strength was 0.1 g kg^{-1} higher in clear-sky conditions than in overcast conditions at Mawson, Davis, and Marambio (not shown). At the other stations, the relationship between cloud cover and surface-based inversion strength was not notable, and hence the decreased strength of all inversions in overcast conditions seen in Fig. 8c was more due to dependency of elevated inversions on cloud cover. The depth of surface-based inversions, on the other hand, was significantly

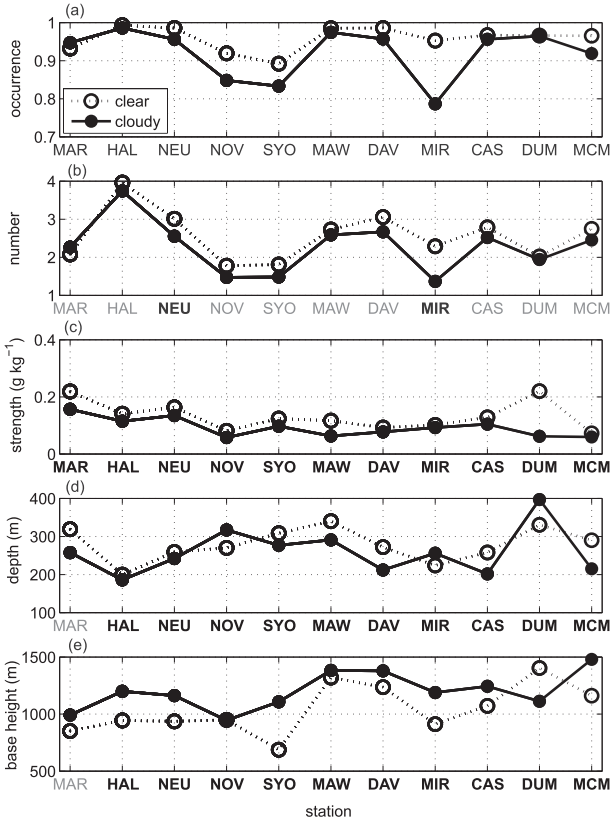

FIG. 8. (a) Occurrence of humidity inversions, (b) mean number of humidity inversions in a profile, (c) median strength, (d) median depth, and (e) median base height of humidity inversions in clear-sky and overcast conditions. The clear-sky cases represent on average 27% of the data and overcast cases 29% of the data at the stations. Stations with statistically significant difference in inversion properties depending on cloud cover are marked with boldface black letters, and stations with no statistically significant difference with gray letters.

higher in overcast conditions, but the depth of elevated inversions was not as consistently influenced by the cloud cover.

Humidity inversion properties were affected by the atmospheric pressure. A connection between humidity inversion occurrence and sea level pressure is shown in Fig. 9. The occurrence was near 1.0 in high pressure conditions, and decreased toward lower pressures. The decrease of inversion occurrence with decreasing pressure was related to both surface-based and elevated humidity inversions, but the connection with the surface-based inversions was stronger. Considering all the inversions, the decrease was statistically significant ($p < 0.05$) at all stations, except for Dumont d'Urville. Furthermore, the median strength and depth of the strongest inversion in the profile slightly increased with pressure, but inversion base height had its maximum at pressures in the middle range.

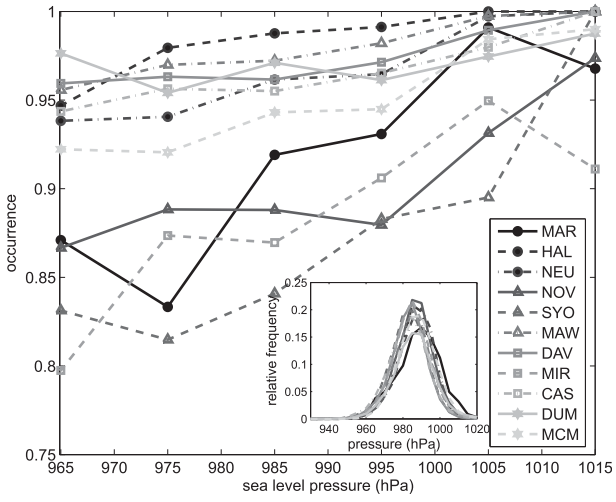

FIG. 9. Dependency between humidity inversion occurrence and sea level pressure. RFDs of sea level pressure are shown in the small figure.

b. *Relationships among humidity inversions, temperature inversions, and moisture transport*

Compared to humidity inversions, temperature inversions occurred slightly more frequently but the number of inversions in a profile was, on average, 1.9 compared to 2.4 for humidity inversions. At all the stations, temperature inversions were generally thinner than humidity inversions, and their median base was found at several hundreds of meters lower than the median base of humidity inversions. In other words, surface-based temperature inversions were much more common than surface-based humidity inversions. Statistical dependency between the humidity and temperature inversion properties is illustrated in Fig. 10 for correlations of temporal variations. Only the strongest humidity and temperature inversion in a profile were considered in Fig. 10. At five stations, humidity and temperature inversion depths were correlated positively and at two stations a connection between temperature and humidity inversion strengths was found. Further, when the temperature inversion was weaker, the humidity inversion base height was typically located at a higher level. This connection suggests that the other formation factors than temperature inversions probably dominate when the temperature inversions in the profile are weak. At three stations, a positive correlation between the humidity inversion strength and depth as well as between the humidity inversion depth and base height were found. This demonstrates how internal properties of humidity inversions are associated with each other. In addition to the above mentioned temporal correlations, some spatial correlations were also

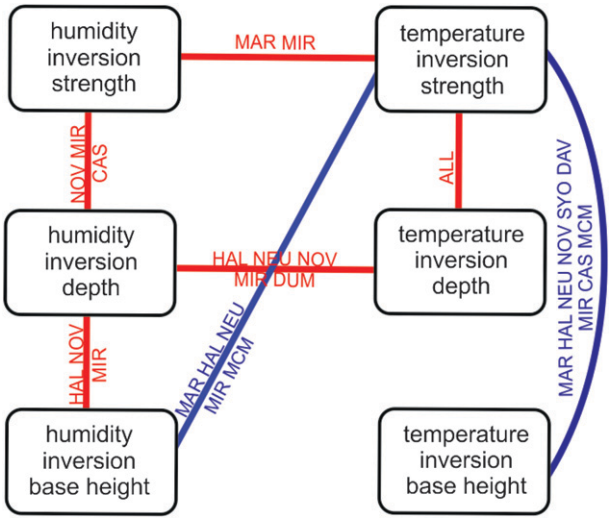

FIG. 10. Schematic figure of temporal dependency between humidity and temperature inversion properties. Only the strongest humidity and temperature inversion in a profile are considered. The red lines denote positive correlation (correlation coefficient r higher than 0.20, $p < 0.01$), and blue lines negative correlation (r lower than -0.20, $p < 0.01$). The stations having a significant correlation are listed.

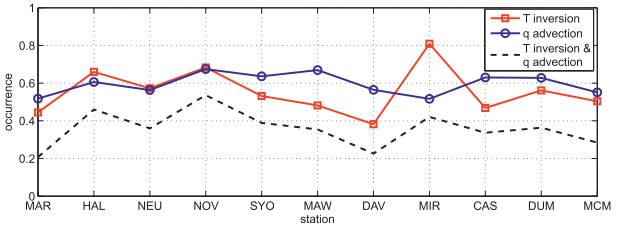

FIG. 11. Occurrence of humidity inversions that transpired simultaneously with a temperature inversion (at least partly within the humidity inversion layer) or with specific humidity advection increasing with height within the humidity inversion layer or with both of them.

found. For example, the humidity inversions were strongest at the stations where the temperature inversions were strongest. Analogously, humidity inversions with a high base were found at the stations with high-based temperature inversions.

Generally, half of all the humidity inversions occurred together with a temperature inversion in all seasons, both near the surface and aloft. This is shown in Fig. 11, which displays the proportion of humidity inversions that had a temperature inversion at least partly within the humidity inversion layer. However, at Mirny the proportion was as high as 0.80. It suggests that a temperature inversion may be the dominant factor supporting a humidity inversion at Mirny. This is in line with Fig. 8, which shows much lower humidity inversion occurrence at Mirny in cloudy conditions than in clear-sky conditions, which is probably connected to the fact that also the occurrence of temperature inversions is lower in cloudy conditions. The potential formation and supporting mechanism of humidity inversions by temperature inversions was introduced in section 1. In addition, the inversion occurrence at Mirny had a clear minimum in summer (Fig. 5), probably due to fewer and weaker temperature inversions. The fact that the soundings were made at different solar time at each station makes an accurate interpretation of spatial differences difficult, as the temperature inversion properties may be affected by the diurnal cycle. Nevertheless, the results generally imply that temperature inversions alone cannot explain the frequent humidity inversions at multiple levels.

Some of the humidity inversions, in all cloud conditions, were associated with water vapor advection. In Fig. 12, median vertical profiles of water vapor advection calculated from the ERA-Interim are shown. For generation of humidity inversions, the vertical change in advection plays a more important role than the absolute magnitudes of water vapor advection. Most of the stations had negative (dry) water vapor advection near the surface, which was likely induced by katabatic winds bringing drier air from inland. However, these katabatic winds simultaneously caused turbulent mixing of the air, as mentioned in section 3a, and this effect compensated for the dry advection. The negative advection generally decreased with height, although individual profiles had highly variable shapes. A few of the stations had a positive (moist) peak in water vapor advection approximately at 1000–2000-m altitude. At Dumont d'Urville, the shape of the water vapor advection profile at 1000–2000 m resembled the specific humidity profile shown in Fig. 4. It thus seems plausible that the humidity advection contributed to the prevailing elevated humidity inversion particularly at Dumont d'Urville. It should, however, be noted that global reanalyses, such as ERA-Interim, are known to have difficulties to simulate the low-tropospheric moisture and thermodynamics over the high latitudes (Bromwich et al. 2011; Bracegirdle and Marshall 2012; Jakobson et al. 2012) and that may affect the advection estimates of the reanalysis.

Within approximately 60% of the humidity inversions, the water vapor advection increased from the inversion base to the inversion top (Fig. 11), and within 30% of inversions this increase was at least 0.2×10^{-5} g kg^{-1} s^{-1}. This means that the vertical increase in water vapor advection was a typical feature of humidity inversion layers and may indicate a way how many of humidity inversions form. Nevertheless, humidity

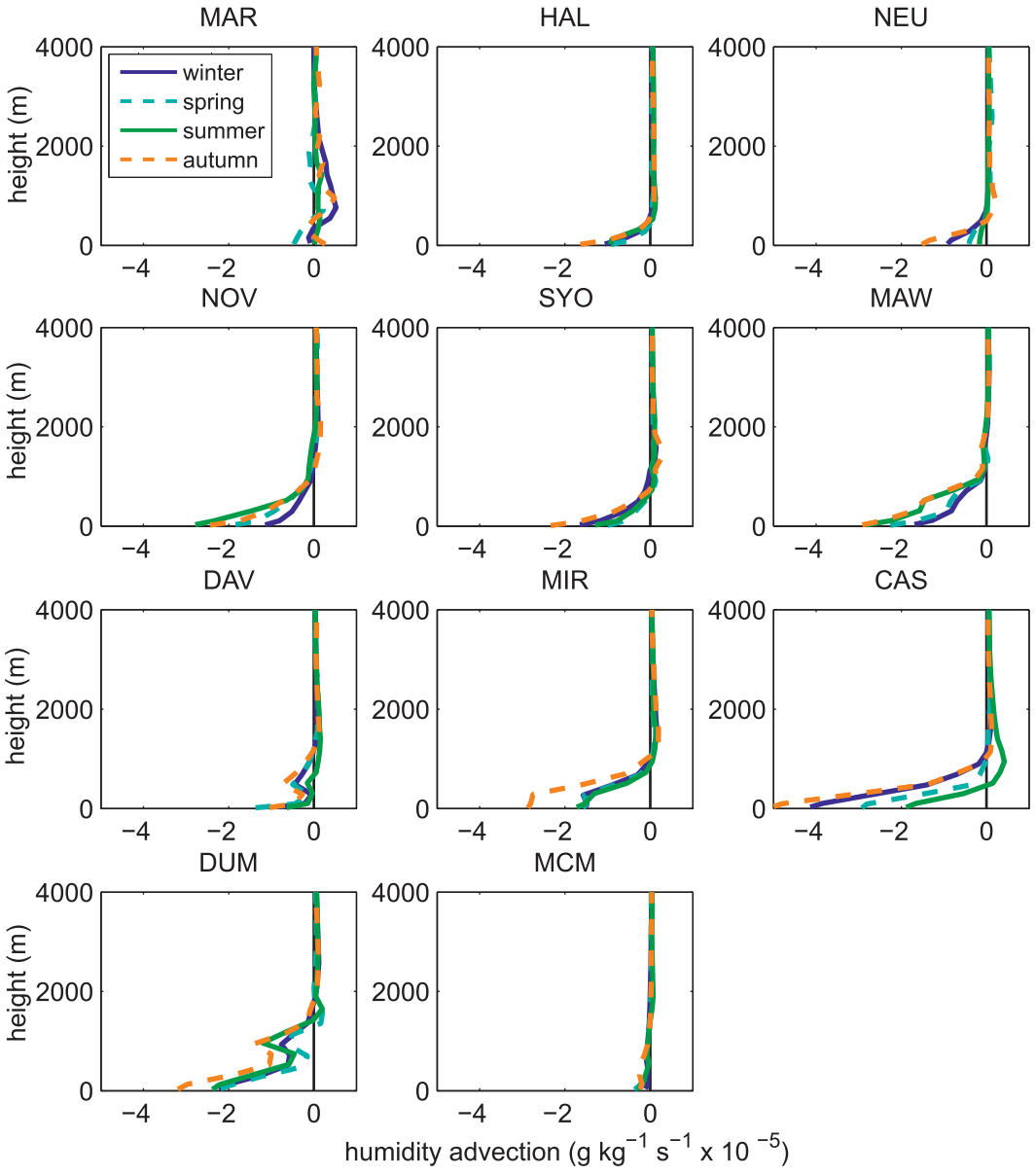

FIG. 12. Seasonal medians of specific humidity advection profiles based on ERA-Interim data. The reanalysis profiles were only included at the times of radio soundings.

inversion strength and the magnitude of vertical change of water vapor advection between the top and base height did not correlate at any station. The vertical increase in water vapor advection within the humidity inversion was least frequent at Mirny, where the humidity inversions were often accompanied by temperature inversions (Fig. 11).

A comparison of the statistical characteristics of the humidity inversions accompanied by a temperature inversion and those accompanied by a vertical increase in water vapor advection revealed clear differences (Fig. 13). It is noteworthy that these categories are partly overlapping. On average, humidity inversions accompanied by a temperature inversion were 0.03 g kg^{-1} stronger, 70 m thinner, and located 440 m lower than the inversions accompanied by a vertical increase in water vapor advection. These kinds of features were found at every station. Although these data categories do not directly tell the true formation or supporting mechanisms of the humidity inversion, the results suggest that humidity inversions linked to a temperature inversion form near the surface, while humidity inversions

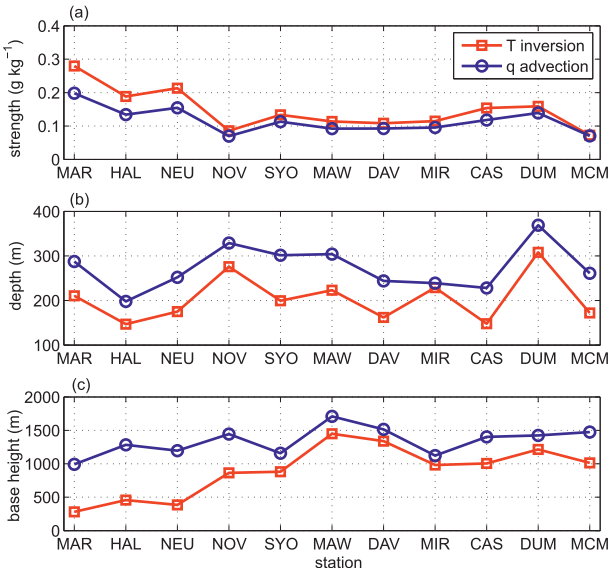

FIG. 13. (a) Median strength, (b) median depth, and (c) median base height of humidity inversions accompanied by a temperature inversion or a vertical increase in water vapor advection.

linked to water vapor advection are weaker but deeper, and higher elevated.

In 36% of the humidity inversions, both a temperature inversion and vertical increase in water vapor advection were found. The occurrence of these inversions was highest at Novolazarevskaya and smallest at Marambio. Temperature inversions and water vapor transport are not independent processes, and the relatively high occurrence of both these features simultaneously suggests that an inversion layer is often affected by several physical processes. In addition, for example, cloud processes alone can create humidity inversions by condensation at cloud top. However, due to absence of reliable data of cloud-top heights, we could not study relationships of the inversion and water vapor transport statistic with the cloud height.

5. Discussion

Our results provide compelling evidence that humidity inversions are very frequent features in the atmosphere of the coastal Antarctic. When only clear-sky conditions are compared, humidity inversion frequency in the Antarctic is even higher than reported by Devasthale et al. (2011) for the Arctic. In wintertime, the difference in the frequencies between the two polar areas is minor, but in summer the difference is clear; according to Devasthale et al. (2011), summertime humidity inversions occur less than 20% of the time in the Arctic, while our results for the Antarctic summer indicated a frequency of more than 70%. Hence, a pronounced seasonal cycle of clear-sky humidity inversion frequency with reduced values in summer is seen in the Arctic but not in the Antarctic. It is, however, noteworthy that clear-sky conditions are not common over the Arctic Ocean in summer, but comparison in all-sky conditions is not possible as the abovementioned statistics by Devasthale et al. (2011) are only based on clear-sky conditions. This prevents solid conclusions on the difference between the Arctic and Antarctic inversion frequencies in all-sky conditions. On the other hand, humidity inversion statistics were not very sensitive to the cloud cover in the Antarctic (see section 4b); therefore, differences between the two polar regions are not expected to be largely affected by cloud conditions. Interestingly, in addition to satellite-derived humidity inversions, Devasthale et al. (2011) also presented results from two Arctic radio sounding stations for all-sky conditions, which in turn showed as high inversion frequencies in summer as in other seasons. This contradiction suggests that part of the difference between the polar areas may, indeed, arise from different instruments, methodologies, and vertical resolutions used to derive the inversion datasets. Other possible explanations for the higher frequency in the Antarctic could be dry katabatic winds related to the complex topography, as well as differences in temperature inversion characteristics and water vapor transport.

Humidity inversion characteristics in the two polar areas have a few clear differences. When only the strongest inversions in the Antarctic are considered, Antarctic inversions are during most of the year roughly twice as strong as Arctic inversions. However, in summer the strongest humidity inversions are nearly equally strong in both polar areas. Interestingly, the seasonal variation of the humidity inversion height differs from the findings of Devasthale et al. (2011); in the Antarctic, the inversions were located at the highest level in summer, not in winter and spring as in the Arctic.

We demonstrated that the surface pressure and cloud cover are associated with humidity inversions in the coastal Antarctic. Relationships between humidity inversion properties and other meteorological variables have earlier been reported by Vihma et al. (2011a) in a study of Arctic fjords. They found strong correlations between humidity inversion properties and low cloud cover as well as variables at 850 hPa, such as temperature, humidity, geopotential height, and wind speed. Both studies support a conclusion that effects of atmospheric pressure and geopotential height on humidity inversions are closely associated with stronger surface-based temperature inversions in high pressure conditions.

In addition, Vihma et al. (2011a) investigated relationships between humidity inversion and temperature inversion properties. They found dependencies between the same properties that we demonstrated in Fig. 10 with red lines. A statistical relationship between the humidity and temperature inversion strengths has previously also been found by Devasthale et al. (2011) in observations from the Arctic, but model simulations of Tastula et al. (2012) for the Antarctic sea ice zone did not show any significant dependency between the humidity and temperature inversion strengths. It could nevertheless be inferred that these relationships between the inversion properties are general features and not specific to a hemisphere or type of topography.

Previous studies based on observational data have, however, not clearly identified contributions of different factors forming and shaping humidity inversions. It is not by any means self-explanatory to determine the contributions, but our results provided insight into potential contributing factors. Roughly half of the humidity inversions had an accompanying temperature inversion, and around 60% of the humidity inversions were accompanied by a vertical increase in water vapor advection. This suggests that both of these factors may be associated with support of humidity inversions in the coastal Antarctic; temperature inversions typically near the surface and advection higher up in the atmosphere. The causal effect of a temperature inversion lies in the removal of water vapor via condensation in the lower (colder) parts of the temperature inversion layer. Humidity and temperature inversions may, however, occur simultaneously also without a direct causal association: they may be generated by a vertical increase in the lateral advection of both heat and moisture. This is the case, for example, during advection of warm, moist marine air masses at upper levels or when katabatic winds advect cold, dry air near the surface but are so weak that not much turbulent mixing is generated (Vihma et al. 2011b). On the other hand, a temperature inversion and a vertical increase of water vapor advection may in many cases be physically connected to each other and possibly also act together to support a humidity inversion. Hence, temperature inversions and water vapor advection cannot be strictly separated. Different statistics of the humidity inversions for the two categories gave evidence to suggest that the mechanism that supports a humidity inversion affects the properties of the inversion. It is noteworthy that the properties of humidity inversions were closer to each other in clear and cloudy conditions than in the two categories related to temperature inversions and a vertical increase of water vapor advection (cf. Figs. 8 and 13). As a summary, the factors generating, supporting, and shaping humidity inversions, discussed either here or in previous studies, are gathered in a schematic illustration in Fig. 14.

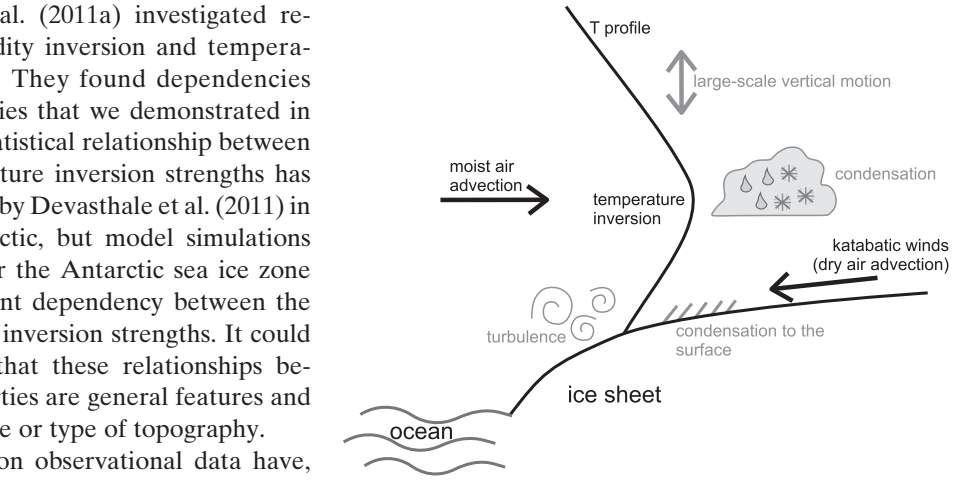

FIG. 14. A schematic presentation of factors forming and shaping humidity inversions. The contribution of factors shown in black was demonstrated in this study while the factors shown in gray have been reported in previous studies.

In the large scale, humidity inversion properties seem to be affected by the spatial variability of the total column water vapor and water vapor flux convergence. Tietäväinen and Vihma (2008) presented a distribution of the water vapor flux convergence in the Antarctic based on the 40-yr ECMWF Re-Analysis (ERA-40). The areas of largest convergence were located near stations Marambio, Casey, Dumont d'Urville, and Syowa. These areas correspond well to the locations with high near-surface specific humidity values (Fig. 3) and to some extent also to the locations with high humidity inversion strength values (Fig. 5). It is, however, noteworthy that a detailed interpretation of the spatial differences is difficult because the solar time of the observations varied significantly from a station to another, and the possible diurnal cycle of humidity inversion properties is not known. The water vapor transport and convergence, in turn, depend on the large-scale circulation patterns (e.g., SAM) (Tietäväinen and Vihma 2008). Consequently, we suggest that oscillations in SAM and other large-scale circulation patterns are likely to cause changes in the humidity inversion properties.

The importance of humidity inversions in the Arctic has been stressed in prior studies, but our results suggest that humidity inversions might have an even more substantial role in the Antarctic climate due to their more frequent occurrence. However, there is still much uncertainty in the implications of the humidity inversions. Our data did not allow for detailed analysis of cloud formation as done by Sedlar et al. (2012) and Solomon

et al. (2011) for the Arctic. For example, because of these limitations it is impossible to know whether the dependency found between the strength of elevated inversions and cloud cover means that humidity inversions are commonly a moisture source for the cloud layer or whether the cloud-top entrainment redistributes specific humidity. On the other hand, our results showed that the number of humidity inversions was slightly reduced in overcast conditions. A probable explanation is that clouds enhance surface warming by emitting longwave radiation, as a consequence of which the near-surface stability is reduced. Near-neutral stability allows mixing out some of the subcloud humidity inversions. This interpretation is supported by the observed increase of humidity inversion base height in overcast conditions (Fig. 8e). In summary, the humidity inversions are a potential moisture source for the clouds also in the Antarctic, but better understanding of this requires further studies based on high-quality cloud data.

Accurate numerical modeling of humidity inversions is challenging. In a way, humidity inversions are a robust metric to evaluate reproducibility of the thermodynamics in the numerical models (Devasthale et al. 2011). To realistically reproduce humidity inversions in the model, water vapor transport, precipitation, temperature, and humidity profiles as well as radiation are required to be accurately captured, but realistic simulation of humidity profiles and clouds is known to be challenging, particularly in the polar areas (Rinke et al. 2006; Fogt and Bromwich 2008). Serreze et al. (2012) and Jakobson et al. (2012) found that observed thermodynamics, including humidity inversions, are not captured by the modern reanalyses in the Arctic. Kilpeläinen et al. (2012) demonstrated that a state-of-the-art mesoscale model could not realistically reproduce humidity inversions. In their study, the model captured only a fraction of humidity inversions over Arctic fjords, whereas, for example, temperature inversions were slightly better captured. In particular, humidity inversions on multiple levels were not at all captured by the model. The results of these studies highlight the need for further studies aiming to improve the thermodynamics in the models.

6. Conclusions

We have quantified the statistical characteristics of humidity inversions using 10 years of radiosonde humidity profiles from 11 coastal Antarctic stations. It is evident from the results that humidity inversions on multiple levels are very common throughout the year. A comparison to previous results for the Arctic revealed that, in clear-sky conditions in summer, the humidity inversions are substantially more common in the Antarctic than in the Arctic. The humidity inversion occurrence in the Antarctic coast increases in high pressure and cloud-free conditions, which often go hand in hand. In addition, the topography of the stations was found to affect the humidity profiles; the stations located on an ice shelf had typically a local minimum of specific humidity near the surface whereas the stations experiencing strong katabatic winds had commonly a specific humidity maximum near the surface. The seasonal variation of inversion strength and depth is relatively small, whereas the inversion base height has notable seasonal variations. The spatial variability of inversion properties, especially inversion strength, is connected to the spatial distribution of near-surface specific humidity, and it also has patterns similar to the water vapor flux convergence estimates presented in previous studies. Both a temperature inversion and a vertical increase in the horizontal water vapor advection are often associated with generation or support of humidity inversions; the former typically near the surface and the latter higher up in the atmosphere. There are, however, notable spatial differences in contributions of these two factors. Presumably, the contribution of the temperature inversions is large, particularly at Syowa, whereas the advection and temperature inversion together have notable roles, especially at Dumont d'Urville. The common existence and potential implications of humidity inversions for clouds and radiation call for further observational and modeling studies. Our results on humidity inversion statistics provide a good baseline for these studies.

Acknowledgments. We are grateful to Steven Colwell (British Antarctic Survey) for providing us with the cloud observations from the Antarctic stations (the READER dataset) and to the anonymous reviewers for valuable comments on the manuscript. This study was supported by the Academy of Finland through the AMICO project (Contracts 128533, 128799, and 263918). ECMWF is acknowledged for providing us the ERA-Interim data. Computing resources of IT Center for Science (CSC) were utilized in this work.

REFERENCES

Bengtsson, L., K. I. Hodges, and S. Hagemann, 2004: Sensitivity of the ERA40 reanalysis to the observing system: Determination of the global atmospheric circulation from reduced observations. *Tellus,* **56A,** 456–471.

Bracegirdle, T. J., and G. J. Marshall, 2012: The reliability of Antarctic tropospheric pressure and temperature in the latest global reanalyses. *J. Climate,* **25,** 7138–7146.

Bromwich, D. H., 1988: Snowfall in high southern latitudes. *Rev. Geophys.,* **26,** 149–168.

——, J. P. Nicolas, and A. J. Monaghan, 2011: An assessment of precipitation changes over Antarctica and the Southern Ocean since 1989 in contemporary global reanalyses. *J. Climate,* **24,** 4189–4209.

——, and Coauthors, 2012: Tropospheric clouds in Antarctica. *Rev. Geophys.,* **50,** RG1004, doi:10.1029/2011rg000363.

Connolley, W. M., and J. C. King, 1993: Atmospheric water-vapour transport to Antarctica inferred from radiosonde data. *Quart. J. Roy. Meteor. Soc.,* **119,** 352–342.

Cullather, R. I., and M. G. Bosilovich, 2011: The moisture budget of the polar atmosphere in MERRA. *J. Climate,* **24,** 2861–2879.

——, D. H. Bromwich, and M. L. Van Woert, 1998: Spatial and temporal variability of Antarctic precipitation from atmospheric methods. *J. Climate,* **11,** 334–367.

Curry, J. A., 1983: On the formation of continental polar air. *J. Atmos. Sci.,* **40,** 2278–2292.

——, W. B. Rossow, D. Randall, and J. L. Shramm, 1996: Overview of Arctic cloud and radiation characteristics. *J. Climate,* **9,** 1731–1764.

Dee, D. P., and Coauthors, 2011: The ERA-Interim Reanalysis: Configuration and performance of the data assimilation system. *Quart. J. Roy. Meteor. Soc.,* **137,** 553–597, doi:10.1002/qj.828.

Devasthale, A., J. Sedlar, and M. Tjernström, 2011: Characteristics of water-vapor inversions observed over the Arctic by Atmospheric Infrared Sounder (AIRS) and radiosondes. *Atmos. Chem. Phys.,* **11,** 9813–9823, doi:10.5194/acp-11-9813-2011.

Durre, I., and X. Yin, 2008: Enhanced radiosonde data for studies of vertical structure. *Bull. Amer. Meteor. Soc.,* **89,** 1257–1262.

——, S. V. Russell, and D. B. Wuertz, 2006: Overview of the integrated global radiosonde archive. *J. Climate,* **19,** 53–68.

Fogt, R. L., and D. H. Bromwich, 2008: Atmospheric moisture and cloud cover characteristics forecast by AMPS. *Wea. Forecasting,* **23,** 914–930.

Giovinetto, M. B., D. H. Bromwich, and G. Wendler, 1992: Atmospheric net transport of water vapor and latent heat across 70°S. *J. Geophys. Res.,* **97** (D1), 917–930.

——, K. Yamazaki, G. Wendler, and D. H. Bromwich, 1997: Atmospheric net transport of water vapor and latent heat across 60°S. *J. Geophys. Res.,* **102** (D10), 11 171–11 179.

Jakobson, E., T. Vihma, T. Palo, L. Jakobson, H. Keernik, and J. Jaagus, 2012: Validation of atmospheric reanalyses over the central Arctic Ocean. *Geophys. Res. Lett.,* **39,** L10802, doi:10.1029/2012gl051591.

Kilpeläinen, T., T. Vihma, M. Manninen, A. Sjöblom, E. Jakobson, T. Palo, and M. Maturilli, 2012: Modelling the vertical structure of the atmospheric boundary layer over Arctic fjords in Svalbard. *Quart. J. Roy. Meteor. Soc.,* **138,** 1867–1883, doi:10.1002/qj.1914.

King, J. C., and J. Turner, 1997: *Antarctic Meteorology and Climatology.* Cambridge University Press, 409 pp.

Medeiros, B., C. Deser, R. A. Tomas, and J. E. Kay, 2011: Arctic inversion strength in climate models. *J. Climate,* **24,** 4733–4740.

Miloshevich, L. M., H. Vömel, D. N. Whiteman, B. M. Lesht, F. J. Schmidlin, and F. Russo, 2006: Absolute accuracy of water vapor measurements from six operational radiosonde types launched during AWEX-G and implications for AIRS validation. *J. Geophys. Res.,* **111,** D09S10, doi:10.1029/2005jd006083.

Ohmura, A., 2001: Physical basis for the temperature-based melt-index method. *J. Appl. Meteor.,* **40,** 753–761.

Pavelsky, T. M., J. Boe, A. Hall, and E. J. Fetzer, 2011: Atmospheric inversion strength over polar oceans in winter regulated by sea ice. *Climate Dyn.,* **36,** 945–955, doi:10.1007/s00382-010-0756-8.

Périard, C., and P. Pettré, 1993: Some aspects of the climatology of Dumont D'Irville, Adélie Land, Antarctica. *Int. J. Climatol.,* **13,** 313–328, doi:10.1002/joc.3370130307.

Rinke, A., and Coauthors, 2006: Evaluation of an ensemble of Arctic regional climate models: Spatiotemporal fields during the SHEBA year. *Climate Dyn.,* **26,** 459–472, doi:10.1007/s00382-005-0095-3.

Sedlar, J., and M. Tjernström, 2009: Stratiform cloud—Inversion characterization during the Arctic melt season. *Bound.-Layer Meteor.,* **132,** 455–474, doi:10.1007/s10546-009-9407-1.

——, M. D. Shupe, and M. Tjernström, 2012: On the relationship between thermodynamic structure and cloud top and its climate significance in the Arctic. *J. Climate,* **25,** 2374–2393.

Serreze, M. C., A. P. Barrett, and J. Stroeve, 2012: Recent changes in tropospheric water vapor over the Arctic as assessed from radiosondes and atmospheric reanalyses. *J. Geophys. Res.,* **117,** D10104, doi:10.1029/2011jd017421.

Slonaker, R. L., and M. L. Van Woert, 1999: Atmospheric moisture transport across the Southern Ocean via satellite observations. *J. Geophys. Res.,* **104** (D8), 9229–9249.

Solomon, A., M. D. Shupe, P. O. G. Persson, and H. Morrison, 2011: Moisture and dynamical interactions maintaining decoupled Arctic mixed-phase stratocumulus in the presence of a humidity inversion. *Atmos. Chem. Phys.,* **11,** 10 127–10 148, doi:10.5194/acp-11-10127-2011.

Tastula, E.-M., T. Vihma, and E. L Andreas, 2012: Evaluation of polar WRF from modeling the atmospheric boundary layer over Antarctic sea ice in autumn and winter. *Mon. Wea. Rev.,* **140,** 3919–3935.

Tietäväinen, H., and T. Vihma, 2008: Atmospheric moisture budget over Antarctica and the Southern Ocean based on the ERA-40 Reanalysis. *Int. J. Climatol.,* **28,** 1977–1995, doi:10.1002/joc.1684.

Tjernström, M., C. Leck, P. O. G. Persson, M. L. Jenssen, S. P. Oncley, and A. Targino, 2004: The summertime Arctic atmosphere: Meteorological measurements during the Arctic Ocean experiment 2001. *Bull. Amer. Meteor. Soc.,* **85,** 1305–1321.

Tomasi, C., and Coauthors, 2006: Characterization of the atmospheric temperature and moisture conditions above Dome C (Antarctica) during austral summer and fall months. *J. Geophys. Res.,* **111,** D20305, doi:10.1029/2005jd006976.

Turner, J., and S. Pendlebury, 2004: *The International Antarctic Weather Forecasting Handbook.* British Antarctic Survey, 663 pp.

Vihma, T., T. Kilpeläinen, M. Manninen, A. Sjöblom, E. Jakobson, T. Palo, J. Jaagus, and M. Maturilli, 2011a: Characteristics of temperature and humidity inversions and low-level jets over Svalbard Fjords in spring. *Adv. Meteor.,* 486807, doi:10.1155/2011/486807.

——, E. Tuovinen, and H. Savijärvi, 2011b: Interaction of katabatic winds and near-surface temperatures in the Antarctic. *J. Geophys. Res.,* **116,** D21119, doi:10.1029/2010JD014917.

Zhang, Y., D. J. Seidel, J. C. Golaz, C. Deser, and R. A. Tomas, 2011: Climatological characteristics of Arctic and Antarctic surface-based inversions. *J. Climate,* **24,** 5167–5186.